Vol. 40 (2009) ACTA PHYSICA POLONICA B No 4

HADRONIC OBSERVABLES FROM Au+Au COLLISIONS AT $\sqrt{s} = 200$ GeV/n AND Pb+Pb COLLISIONS AT $\sqrt{s} = 5.5$ TeV/n FROM A SIMPLE KINEMATIC MODEL*

T.J. Humanic

Department of Physics, The Ohio State University, Columbus, Ohio, USA

(Received February 4, 2009)

A simple kinematic model based on superposition of $p+p$ collisions, relativistic geometry and final-state hadronic rescattering is used to calculate various hadronic observables in $\sqrt{s} = 200$ GeV/nucleon Au + Au collisions and $\sqrt{s} = 5.5$ TeV/nucleon Pb + Pb collisions. The model calculations are compared with experimental results from several $\sqrt{s} = 200$ GeV/nucleon Au + Au collision studies. If a short hadronization time is assumed in the model, it is found that this model describes the trends of the observables from these experiments surprisingly well considering the model's simplicity. This also gives more credibility to the model predictions presented for $\sqrt{s} = 5.5$ TeV/nucleon Pb + Pb collisions.

PACS numbers: 25.75.Dw, 25.75.Gz, 25.40.Ep

1. Introduction

The experiments at the Relativistic Heavy Ion Collider (RHIC) have produced many interesting studies of hadronic observables from relativistic heavy-ion collisions over the past six or so years. The goal has been to use these observables to characterize the conditions of the early state of matter in heavy-ion collisions so as to be possible signatures of exotic states, such as Quark Matter. Models which describe the early stages of the collision after the initial nuclei have passed through each other in terms of partonic degrees of freedom, for example as a cascade or in terms of hydrodynamics, have been successful in describing the experimental systematics of some of these observables in some kinematic ranges, but no single model has thus far succeeded in making an adequate overall description of the systematics of all of these observables in a wide kinematical range.

* Presented at the IV Workshop on Particle Correlations and Femtoscopy, Kraków, Poland, September 11–14, 2008.

The goal of the present work is to see how far one can get in describing the experimental systematics of all of the observables mentioned above in a wide kinematical range using a simple kinematic model with hadronic degrees of freedom. In essence the model is, for each heavy-ion collision, a superposition of $p+p$ collisions in the geometry of the colliding nuclei with a proper time for hadronization determining the initial space-time position of each produced particle, followed by a Monte Carlo hadronic rescattering calculation. The $p+p$ collisions are generated by the PYTHIA code [1] at the beam energy of interest.

There is no *a priori* reason why such an approach should be successful, and in fact there are reasons to think it should be unsuccessful, the most serious one being that it is hard to imagine that hadronic degrees of freedom, rather than partonic degrees of freedom, can be valid soon after the nuclei have passed through each other due to the expected high energy density. This would require a very short hadronization time in these collisions. On this point, it is encouraging that a recent study of pion HBT in Tevatron collisions has shown that a similar model for $p+p$ collisions can explain the p_{T} and multiplicity dependences for the extracted radius parameters if a very short proper time for hadronization of 0.1 fm/c is assumed [2] This assumption for the proper time is also made in the present work.

Model calculations will be compared with results from RHIC experiments for Au + Au collisions at $\sqrt{s} = 200$ GeV/nucleon. The goal will be to make as quantitative comparisons as possible between model and experiments. Predictions from the model for LHC-energy Pb + Pb collisions at $\sqrt{s} =$ 5.5 TeV/nucleon will also be given.

The model calculations are carried out in five main steps: (A) generate hadrons in $p+p$ collisions from PYTHIA, (B) superpose $p+p$ collisions in the geometry of the colliding nuclei, (C) employ a simple space-time geometry picture for the hadronization of the PYTHIA-generated hadrons assuming a proper time for hadronization of 0.1 fm/c, (D) calculate the effects of final-state rescattering among the hadrons, and (E) calculate the hadronic observables. These steps are discussed in detail elsewhere [3].

2. Results from the model

A sample of hadronic observables have been calculated from a 87K minimum bias run from the model and are compared with measurements from RHIC experiments below. More results from this work are shown elsewhere [3]. In the spirit of making as quantitative comparisons as possible between model and experiments, unless explicitly specified otherwise, absolute normalizations are used for the model observables in the plots shown.

Figures 1 and 2 show comparisons between the model and experiments for elliptic flow. Figure 5 compares the model to PHOBOS for charged particles for V_2 *versus* η in a centrality window of 25–50% [4]. The model is seen to agree with the measurements within error bars for the entire range in η, *i.e.* $-6 < \eta < 6$, although it looks systematically about 10% lower than experiment around mid-rapidity. Note that in the model, V_2 is completely determined by rescattering such that if the rescattering is turned off, $V_2 = 0$ in all kinematic regions.

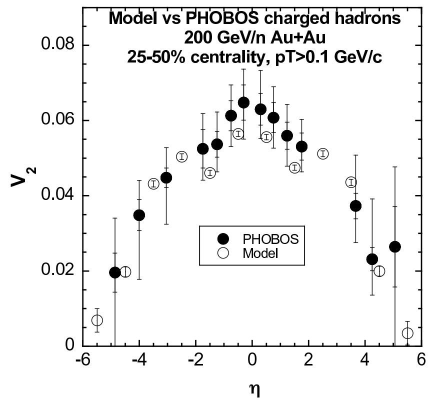

Fig. 1. V_2 *versus* η for Model compared with PHOBOS 25–50% centrality.

Figure 2 compares the model with STAR for V_2 *versus* $p_{\rm T}$ for charged particles in a centrality bin 10–40% in a wide $p_{\rm T}$ range, *i.e.* $p_{\rm T} < 6$ GeV/c [5]. What is remarkable about this comparison is that the model describes the $p_{\rm T}$ behavior of the experiment in which V_2 increases for $p_{\rm T} < 2$ GeV/c, flattens out, and then starts decreasing for $p_{\rm T} > 3$ GeV/c. Once again, this behavior is completely rescattering-driven in the model.

Figure 3 shows plots for identified particles in terms of the number of valance quarks in the identified particle, n_q, as V_2/n_q *versus* $p_{\rm T}/n_q$ and compared with PHENIX [6]. The point of doing this is to show that the different identified particles follow a universal curve when plotted on the same graph this way. Not surprisingly in the context of the discussion above, the model is seen to follow the experimental scaling quantitatively for $p_{\rm T}/n_q < 1$ GeV/c and qualitatively at a lower value for $p_{\rm T}/n_q > 1$ GeV/c.

For the HBT calculations from the model, the three-dimensional two-pion correlation function is formed and a Gaussian function in momentum difference variables is fitted to it to extract the pion source parameters. Boson statistics are introduced after the rescattering has finished (*i.e.* when all particles have "frozen out") using the standard method of pair-wise symmetrization of bosons in a plane-wave approximation [7]. Figure 4 shows

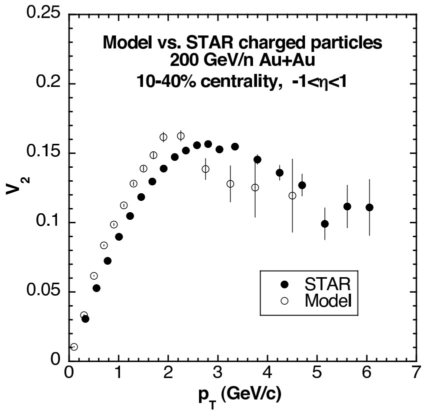

Fig. 2. V_2 *versus* p_{T} for Model *vs* STAR for charged particles and up to high p_{T}.

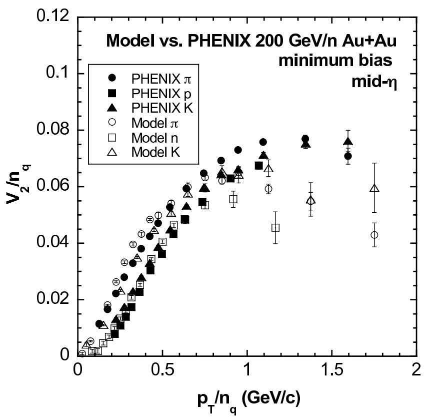

Fig. 3. V_2/n_q *versus* p_{T}/n_q for Model *vs* PHENIX for pions, kaons, and protons.

comparisons between the model and STAR for radius parameters extracted as a function of azimuthal angle, ϕ, for the centrality cut 40–80% [8]. The model describes the oscillatory behavior seen in R_{out} and R_{side} as well as R^2_{outside} and the flat dependence seen in R_{long}, although under predicting the magnitude of R_{side} by about 30%. The λ-parameters extracted in the fits from the model were constant in ϕ with the value 0.54.

Studying the high p_{T} behavior of the observables R_{AA} and $dn/d\Delta\phi$ is thought to be a way of more directly studying QCD processes, such as jets, in heavy-ion collisions. Since the present model is based on using PYTHIA which uses QCD processes in calculating $p+p$ collisions, the model should contain these effects and thus should be suitable for comparing with experiments which measure these observables.

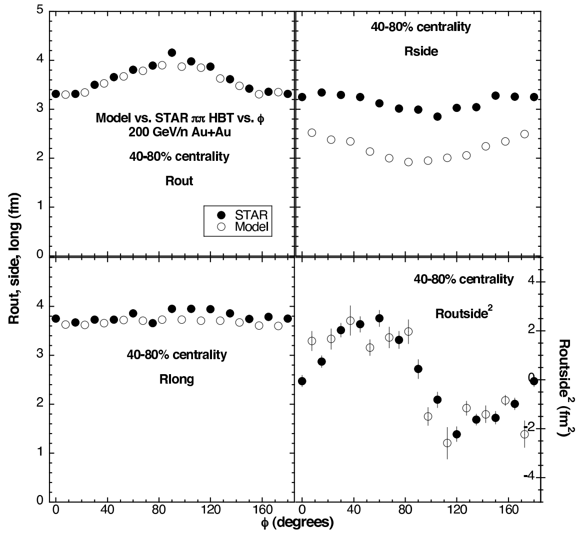

Fig. 4. Azimuthal two-pion HBT parameters *versus* ϕ from Model *vs* STAR for centrality 40–80%.

Figure 5 compares the model to PHENIX for R_{AA} *versus* p_{T} for three centrality windows [9]. The error bars shown for the PHENIX plots are a sum of both statistical error and the overall scale uncertainty, and they mostly reflect the scale uncertainty. As seen, the model describes three main qualitative features of the experiment: (1) for large p_{T} the R_{AA} decreases with increasing p_{T}, and as the centrality window goes from minimum bias (0–92%) to peripheral (80–92%), (2) the scale of R_{AA} increases, and (3) the dependence of R_{AA} on p_{T} tends to flatten out. It is also seen that, even with the uncertainty in the PHENIX overall normalization, the model scale tends to be lower than experiment, and at low p_{T} the peaks in the plots for the model occurs at about 1.3 GeV/c whereas the peaks occur at about 2.3 GeV/c for experiment.

Figure 6 shows $dn/d\Delta\phi$ *versus* ϕ plots from the model and a comparison of one of them with STAR charged particles [10]. The model plots, which include all hadrons, are made using the same cuts on rapidity and p_{T} as used by STAR, namely for individual particles $|\ \eta\ |< 0.7$ and $p_{\mathrm{T}} > 2$ GeV/c, and for particle pairs, one of which is a "trigger particle", from which $\Delta\phi$ is formed, $|\ \Delta\eta\ |< 1.4$ and $p_{\mathrm{T}}^{\mathrm{Trig}} > 4$ GeV/c. The lines are fits to the model points to guide the eye. A more central case from the model is shown in Fig. 6(d) where the centrality window is 0–10%. Although this plot is pushing the edge of the statistics possible from the 87K event model run used in this study for 200 GeV/n Au + Au collisions, it appears to have a qualitatively different shape compared with the other plots shown in this

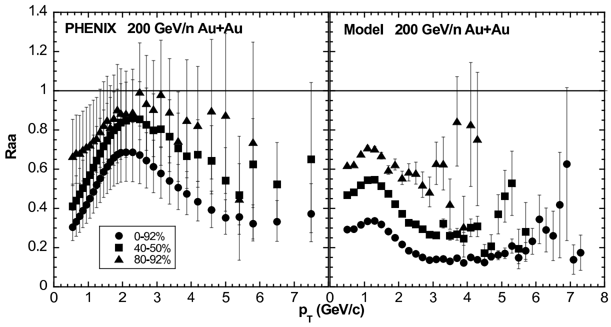

Fig. 5. R_{AA} for Model compared with PHENIX for several centralities.

figure. Namely, besides the presence of the forward peak, the plot looks more or less flat for values of $\Delta\phi$ out to $\pm\pi$, *i.e.* the backward peak appears suppressed. This is the same general behavior seen in STAR in the same centrality window, *i.e.* Fig. 1(c) of Ref. [10].

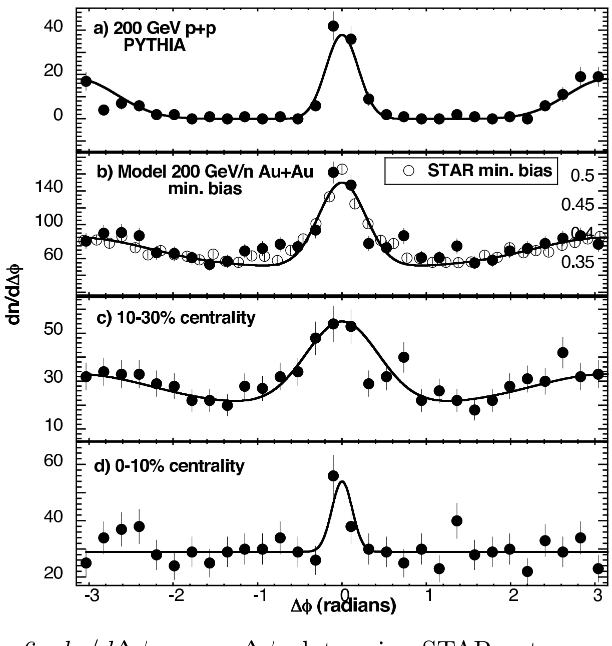

Fig. 6. $dn/d\Delta\phi$ *versus* $\Delta\phi$ plots using STAR cuts on p_{T}.

Figures 7 and 8 show the sample model predictions from a 800 event minimum bias run for 5.5 TeV/n Pb + Pb collisions compared with 200 GeV/n Au + Au collisions, also from the model.

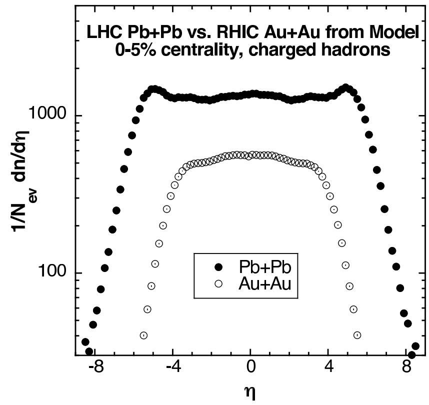

Fig. 7. Rapidity distributions from Model comparing $\mathrm{Pb} + \mathrm{Pb}$ collisions at $\sqrt{s} = 5.5$ TeV/n (LHC) with $\mathrm{Au} + \mathrm{Au}$ collisions at $\sqrt{s} = 200$ GeV/n (RHIC) for charged particles and 0–5% centrality.

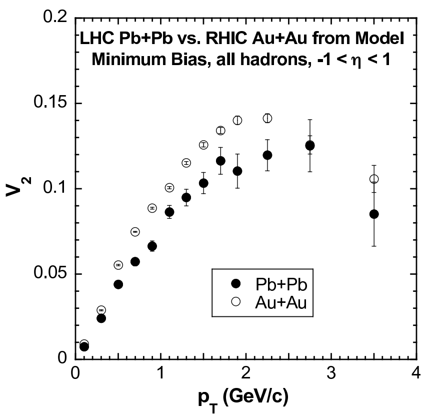

Fig. 8. V_2 *versus* p_{T} from Model comparing LHC $\mathrm{Pb} + \mathrm{Pb}$ with RHIC $\mathrm{Au} + \mathrm{Au}$ collisions; minimum bias centrality, all hadrons, and $-1 < \eta < 1$.

3. Summary and conclusions

As shown above, the main strength of the present model is not that it gives precise agreement with experiment for individual observables in particular kinematic regions, but in its ability to give an overall qualitative description of a range of observables in a wide kinematic region, *i.e.* to summarize the gross features seen in experiments for $\sqrt{s} = 200$ GeV/n $\mathrm{Au} + \mathrm{Au}$ collisions. Another strength is its simplicity. Besides the kinematics generated in the superposed $p + p$ collisions by PYTHIA, the only other "active ingredient" in the model driving the kinematics underlying the hadronic observables shown is the final-state hadronic rescattering.

The author wishes to acknowledge financial support from the U.S. National Science Foundation under grant PHY-0653432, and to acknowledge computing support from the Ohio Supercomputing Center. The author also wishes to acknowledge enlightening discussions related to this work with Hans Bøggild, Ole Hansen and Boris Tomasik.

REFERENCES

[1] T. Sjostrand, L. Lonnblad, S. Mrenna, P. Skands, *J. High Energy Phys.* **0605** 026 (2006) [arXiv:hep-ph/0603175].

[2] T.J. Humanic, *Phys. Rev.* **C76**, 025205 (2007).

[3] T.J. Humanic, arXiv:0810.0621 [nucl-th].

[4] B.B. Back *et al.* [PHOBOS Collaboration], *Phys. Rev.* **C72**, 051901 (2005)

[5] B.I. Abelev *et al.* [STAR Collaboration], *Phys. Rev.* **C77**, 054901 (2008).

[6] A. Adare *et al.* [PHENIX Collaboration], *Phys. Rev. Lett.* **98**, 162301 (2007).

[7] T.J. Humanic, *Phys. Rev.* **C34**, 191 (1986).

[8] J. Adams *et al.* [STAR Collaboration], *Phys. Rev. Lett.* **93**, 012301 (2004).

[9] S.S. Adler *et al.* [PHENIX Collaboration], *Phys. Rev.* **C69**, 034910 (2004)

[10] C. Adler *et al.* [STAR Collaboration], *Phys. Rev. Lett.* **90**, 082302 (2003).